2 DOF Passive Haptic Display with Redundant Actuation for Increase in Force Manipulability Ellipsoid

Chang-hyun Cho[1], Munsang Kim[2], Jae-Bok Song[3]

[1,2] KIST Advanced Robotics Research Center, Hawolgok-dong Sungbuk-gu, Seoul, Korea
+82-2-958-6744, Fax: +82-2-958-5629
[1] chcho@kist.re.kr, [2] munsang@kist.re.kr
[1, 3] Dept. of Mechanical Engineering, Korea University, Seoul, Korea
[3]jbsong@korea.ac.kr

Abstract

In this paper the problems of a force display device equipped with energy dissipative actuators such as a brake or a damper are discussed. This kind of problem can be investigated by considering a force manipulability ellipsoid (FME). The direction in which a Cartesian force can be generated on the FME in a typical 2-link manipulator with passive actuators is very limited compared to the manipulator equipped with motors. To overcome this problem a redundantly actuated passive 2-link manipulator is proposed in this research. By adopting either direct drive or coupled wire drive, the region in which force display is possible can be extended.

1. Introduction

The advance of virtual reality and robotic operation requires man-machine interface to cyber-space or real-space for many applications such as game and teleoperation. Most of physical man-machine interface devices like a joystick and a master arm have recently been equipped with haptic display capability. The haptic display is generally used in terms of force display, which implies both kinesthetic and tactile feedback, though its exact meaning is tactile feedback.

Haptic display devices generally use an electric motor as a force or torque generating actuator. The use of active elements leads to many problems on the control scheme because motors can generate supplementary energy to both a human operator and its feedback environments. Passivity control schemes for reducing internal energy in a haptic device are sometimes used for motor-driven haptic display devices in [1] and [4]. [1] proposed the passivity observer and passivity controller on input and output ports of a haptic device. Even though stability problems of haptic devices with active elements can be partly solved using various control schemes, there remain mechanical problems due to size and weight of active actuators.

It was claimed in [3] that a brake can provide very hard constraints but it poses difficulty in control owing to its passive characteristics. A nonholonomic haptic display adopting the constraint of wheel (i.e. a wheel cannot rotate in the axial direction) is presented on [3]. [6] used four dry friction clutches as a haptic actuator for a 2DOF planar haptic display and showed path following capability through experiments. The device has two redundant DOFs in actuation by the additional two clutches, which changes power flow. [2] showed succeeded research of [6] on application to an obstacle avoidance. [2] presents the single degree of freedom controller (SDOF Controller), which uses Single DOF (SDOF) line achieved by locking one clutch to reduce a system DOF. Thus the proposed system has four SDOF lines and defined an obstacle with the four SDOF lines. [5] used adjustable latch with motor to limit joint velocity and describes environments with tiled section.

Problems and difficulties of passive haptic displays are listed as follow:

- Cannot cover all force directions [6], [2]
- Discrete haptic display [3], [2]

While previous researches addressed limitations of a passive haptic display, no one claimed what the limitation is and which direction is possible to a given kinematic configuration. In this paper, we start with force manipulability analysis of a typical 2-link manipulator to find characteristics of a passive haptic display.

Force manipulability means force generating capability of a manipulator in task (or operational) space [8]. To systematically represent this capability, a so-called force manipulability ellipsoid (FME) is usually employed. An FME is a graphical representation of producible forces in task space for a given kinematic configuration. In the FME for a manipulator equipped with passive actuators such as a brake and a damper, the FME can be divided into the regions in which force displays are available and are not unlike the FME for a manipulator with active actuators such as a motor. To overcome this problem of limited range of force display, a 2-link redundantly actuated manipulator is proposed in this research. This manipulator is operated in either direct drive mode or coupled wire drive mode in order to maximize the range of force display.

The rest of the paper is organized as follows. Section 2 presents an FME analysis for a typical 2-link manipulator. A redundantly actuated 2-link manipulator is introduced in Section 3. Conclusions are drawn in Section 4.

2. FME Analysis for 2-Link Manipulator

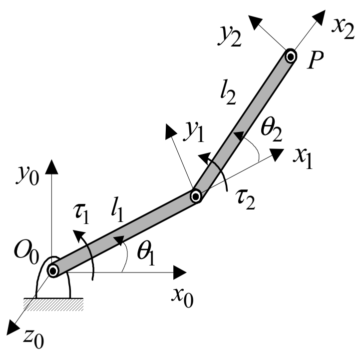

Fig. 1 2-link manipulator

Figure 1 shows a typical 2-link manipulator, where link frames and joint angles θ_1 and θ_2 are defined according to Denavit-Hartenberg representation. It is assumed that the actuators – motors or brakes - are directly attached on each joint. When the manipulator is driven with active actuators such as an electric motor, the tip P can generate tip force $\mathbf{F}$ in any direction in task space (or operational space) and thus a force manipulability ellipsoid (FME) becomes a full ellipsoid. The joint torque vector $\boldsymbol{\tau}$ is computed by $\boldsymbol{\tau} = \mathbf{J}(\mathbf{q})^T \mathbf{F}$, where $\mathbf{J}$ is the Jacobian matrix and $\mathbf{q}$ is the joint variable vector (i.e., $\mathbf{q} = [\theta_1 \ \theta_2]^T$ for a 2-link manipulator) . A FME is then defined as

$$\mathbf{F}^T \mathbf{J}\mathbf{J}^T \mathbf{F} \le 1 \quad \text{s.t.} \|\boldsymbol{\tau}\| \le 1 \tag{1}$$

That is, the FME is obtained by imposing the condition of $\|\boldsymbol{\tau}\| = 1$, from which the joint torque vector can be described by

$$\boldsymbol{\tau} = [\cos(\phi) \quad \sin(\phi)]^T \tag{2}$$

where ϕ is an angle between 0 and 2π.

Equation (1) shows that only joint variables and joint torques are required to plot an FME for the manipulator with active actuators (will be called "active FME" for convenience). However, an FME for the manipulator equipped with passive actuators such as a brake or a damper is determined by joint velocities as well as joint variables and torques. The joint velocities are needed to take into account passive characteristics of a passive actuator since the passive device can provide a torque only against the joint velocity. The torque generated by a brake for the 2-link manipulator can be given by

$$^P\tau_i = \begin{cases} -\text{sgn}(\dot{\theta}_i)\,|\tau_i| & \text{if } \text{sgn}(\dot{\theta}_i) \ne \text{sgn}(\tau_i) \\ 0 & \text{else} \end{cases} \quad (i = 1, 2) \tag{3}$$

where sgn(x) > 0 for x >0, sgn(x) < 0 for x < 0 and sgn(x) = 0 for x = 0. In Eq. (3), $^P\tau_i$ denotes the torque by a passive device and the subscript i represents the joint number. Then the passive FME (an FME created by the manipulator with passive actuators) can be obtained from Eq. (1) by taking Eq. (3) into account.

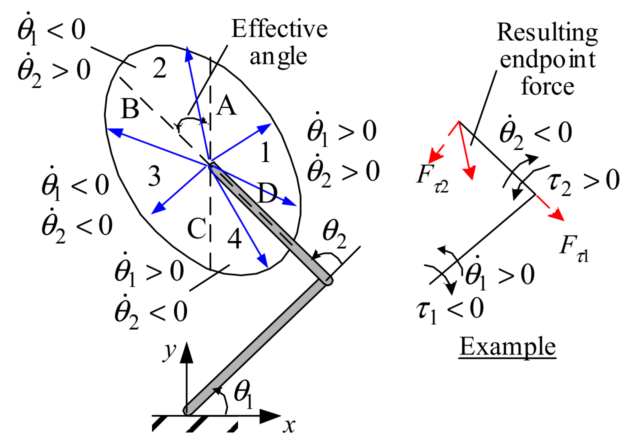

Fig. 2 Passive FME

Figure 2 shows the passive FME for a given configuration (in this case, θ_1 = 45°, θ_2 = 90°). Unlike the active FME, it can be divided into 4 regions. For example, suppose $\dot{\theta}_1 > 0$ and $\dot{\theta}_2 < 0$ as shown in the example in Fig. 2. Then the torques τ_1 and τ_2 should be applied in the CW and CCW respectively, so the resulting tip force is limited to region 4 in Fig. 2. This means that for the given condition of joint velocities, haptic force display is available in Region 4. Likewise, 4 regions delimited by lines A and B are determined depending on the sign of each joint velocity. In Fig. 2 an angle between lines A and B is termed as an effective angle. The number of regions can be given by

$$n_S = 2^{n_O} \tag{4}$$

where n_O is the number of DOFs of task space (2 in this case) and n_S is the number of regions. This equation is also applicable to kinematically redundant systems such as a 3-

link planar manipulator (in case only translational variables *x* and *y* are considered).

To help understanding of a passive FME, let us take another example. Suppose one wants to generate the force in +*x* direction (i.e. region 1), while the tip of the manipulator is moving in –*y* direction. This motion is possible when $\dot{\theta}_1 < 0$ and $\dot{\theta}_2 > 0$, thus corresponding to region 2 in Fig. 2. Therefore, creating the force in +*x* direction is not possible since the angle between the line A of region 2 and +*x* direction is 90° in a given configuration. Next, suppose the force in –*x* direction is needed for the same situation. In this case the angle between the line B of region 2 and -*x* axis becomes 45° (< 90°). If the force is generated along line B, the component of this force can be directed in the –*x* axis and thus the desired force can be roughly displayed, although the unnecessary force is inevitably created in other directions. Again such situations do not occur for an active FME. The above argument graphically shows limitation of a passive haptic display, which was briefly mentioned on [2], [3] and [6].

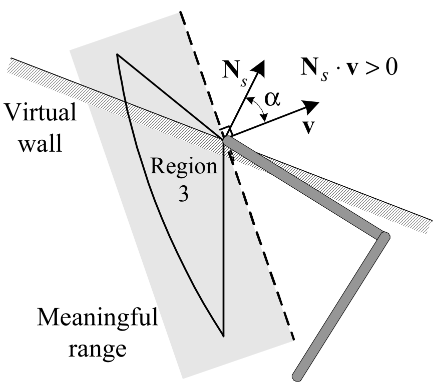

(a) $\mathbf{N}_s \cdot \mathbf{v} > 0$

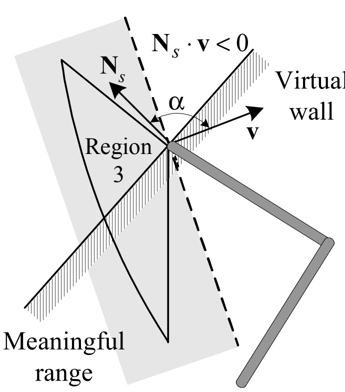

(b) $\mathbf{N}_s \cdot \mathbf{v} < 0$

Fig. 3 Haptic display for Virtual wall

When the environment is passive, there is no need to cover the entire range for haptic display. Fig. 3 shows an application of a passive haptic display to a virtual wall that is a typical passive environment. In this situation it is assumed that the joint velocities are such that $\dot{\theta}_1 < 0$ and $\dot{\theta}_2 < 0$, thus implying region 3. The vector $\mathbf{N}_S$ is a surface normal of a virtual wall and **v** is a unit vector in the direction of the tip motion. The dashed line indicates the boundary of a meaningful range (shaded area) for a haptic display for passive environment, which is the line normal to **v**. In the case (a), $\mathbf{N}_S$ is placed outside the meaningful range and thus haptic display is not required since the tip moves toward the free space. Mathematically, the situation occurs when the inner product $\mathbf{N}_s \cdot \mathbf{v} > 0$. In the case (b), $\mathbf{N}_s$ is placed inside the meaningful range (i.e., $\mathbf{N}_s \cdot \mathbf{v} < 0$) and thus haptic display is required since the tip moves toward the inside of the virtual wall. By checking the sign of the inner product, necessity of haptic display can be determined.

3. Redundant Actuation with Coupled Wire Drive

A wire drive is a simple and widely used power transmitting mechanism. Fig. 4 shows two types of wiring, where P_1 and P2 are input and output pulley, respectively. Each arrow represents the direction of rotation.

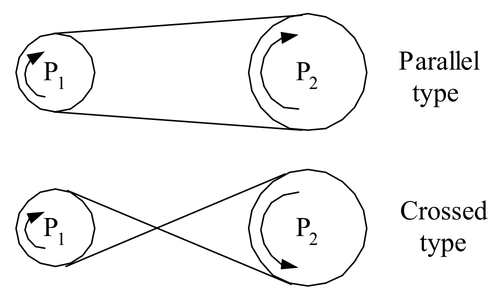

Fig. 4 Types of wire transmission

Fig. 5 shows a 2-link passive manipulator equiped with brakes. In a typical case, only brakes B_1 and B_2 are mounted and the links are directly driven by these brakes. However, the proposed passive manipulator has an additional brake B_3 which is connected to link 2 through parallel wiring. In this mechanism the pulley P_1 is placed on the base and P_2 is fixed on the link 2. The motion of link 2 can be affected by either B_2 or B_3. The power transmission method is called a direct drive when link 2 is driven by B_2, and called a coupled wire drive when it is driven by B_3. It is assumed that in any drive only one brake (i.e., either B_2 or B_3) is applied. Note that the discussion in Section 2 is for direct drive.

In case of direct drive, the joint angle θ_2 is the same as the angle of B_2 because of direct drive between B_2 and joint 2. When coupled wire drive is in action, the joint angle θ_2 is given by

$$\theta_2 = +k\theta_3 - k\theta_1 \quad (5a)$$

for parallel wiring, or

$$\theta_2 = -k\theta_3 + k\theta_1 \quad (5b)$$

for crossed wiring, where θ_3 is a rotation angle at the brake B_3 and k (> 0) is a reduction ratio of a wire drive. This can be explained from the example in Fig. 5(b). For easy understanding, suppose all brakes are replaced by motors. From the initial configuration with θ_1 = 0 and θ_3 = 0, B_3 rotates to θ_3 = 45° (thus θ_2 = 45°) with B_1 locked. After releasing B_1, Then B_1 rotates to θ_1=90° with B_3 locked. The resultant configuration is described by θ_2 = -45°, which can be predicted by Eq. (5a) except for reduction ratio k (in this example k = 1). Note that the wire can move relative to the pulley although the pulley P_1 is locked by brake B_3. This concept can be easily extended to the case of brakes. This type of motion by coupled wire drive can create a partially active property on joint 2, which is the main reason for using a redundant actuation scheme.

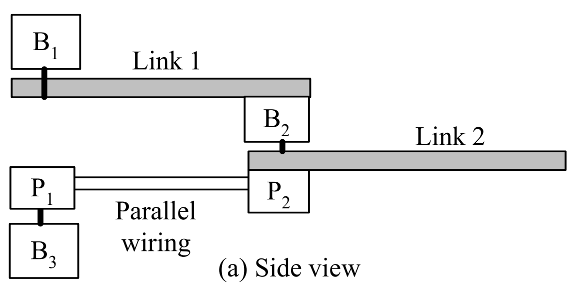

(a) Side view

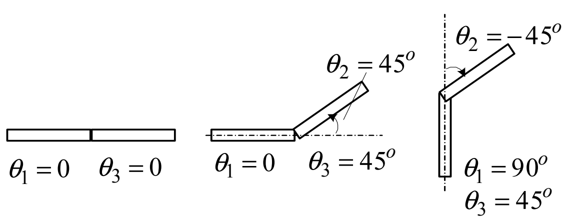

(b) Example of coupled motion

Fig. 5 Redundantly actuated system and resulting motion

Redundant actuation in Fig. 5(a) is accomplished with superposition of a coupled wire drive (i.e., B_3 in action) of parallel type and a direct drive (i.e., B_2 in action). The redundant actuation gives two FMEs, which are the FME from the direct drive and the FME from the coupled wire drive. Two resulting FMEs extend the effective angle of the usable FME by combining them.

The passive FMEs of the redundantly actuated manipulator are presented on Fig. 6. The vector **v** is a unit vector in the direction of tip motion. The dotted ellipsoid is the passive FME for the direct drive mechanism and the dash-dot ellipsoid represents that of the coupled wire drive mechanism. Fig. 6 illustrates all possible combinations of the two FMEs for several velocity vectors **v** on a given configuration (i.e., θ_1 = 45°, θ_2 = 90°). By redundant actuation, the effective angle lies in the range of 90° ~ 135° range, although the effective angle of the direct drive mechanism is in the range of 45° ~ 135°. An increase in the minimum effective angle is 45° from the numerical point of view, but more important function of the redundant actuation is found in Fig. 6. In case of Fig. 6(c) or (f), the effective angle is extended to 135° with the introduction of the coupled wire drive, while that of the direct drive manipulator only covers 45°. The net increase in the effective angle is 0° ~ 90° depending on the direction of the tip motion for this configuration. The effective angle of the direct drive manipulator holds 45° in Fig. 6(b), (c), (e) and (f) and it is the worst case of the direct drive manipulator for haptic display. By redundant actuation, therefore, half of the worst cases can be eliminated.

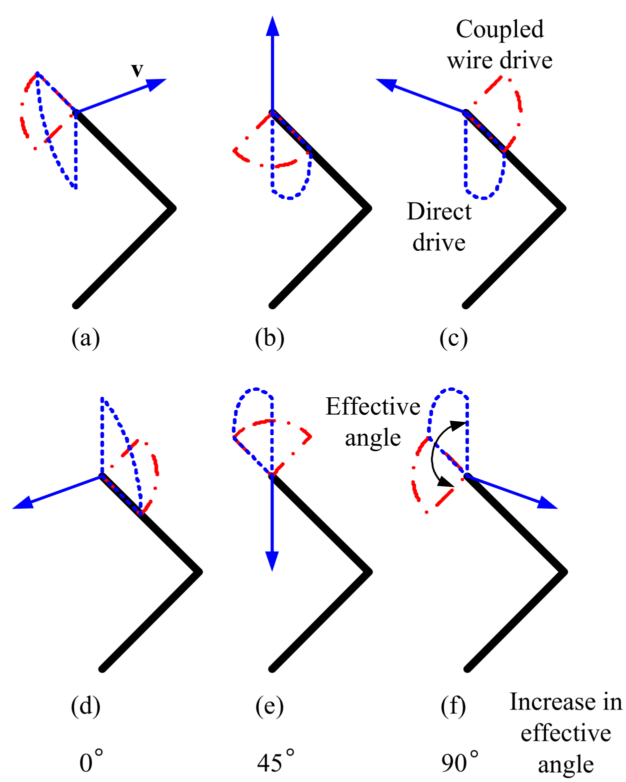

Fig. 6 Passive FME of redundantly actuated system

Although the range of force display can be extended, a problem of displaying approximated force discussed on Section 2 still exists as shown in Fig. 6 (b) and (e) (i.e., the effective angle is 90°). The angle between any line of cut and the desired force direction lies within the range of 0 ~

90^o in Fig. 6(b) and (e), while those for other cases are in the range of 0 ~ 45^o. As explained earlier, the approximation angle in the range of 45 ~ 90^o range may provide a poor quality of haptic display. In particular, at an angle of 90^o, the force cannot be reflected at all.

5. Conclusion

A redundantly actuated 2-link manipulator is presented for a passive haptic display. A passive force manipulability ellipsoid (FME) is obtained by applying the passive characteristic to a general FME and gives a clear view of limitation for a passive haptic display. The effective and meaningful angles are defined on the passive FME and are used to verify possibility of the given mechanism to apply passive force reflection to the passive environment. An additional brake is attached on the second joint of a general 2-link manipulator with parallel type wire drive to compensate for the limitation given by the passive FME. Redundant actuation enlarges the effective angle to remain in the range of 90°~ 135°. The largest net increase in effective angle by redundant actuation is 90°.

References

[1] B. Hannaford, J.-H. Ryu, “Time Domain Passivity Control of Haptic Interfaces”, Proc. of the IEEE Int. Conf. on Robotics & Automation, pp. 1863-1869.

[2] D. K. Swanson, W. J. Book, “Obstacle Avoidance Methods for a Passive Haptic Display,” Proc. Of the IEEE Int. Conf. On Advanced Intelligent Mechatronics, pp. 1187-1192, 2001.

[3] J. E. Colgate, M. A. Peshkin, W. Wannasuphoprasit, “Nonholonomic Haptic Display,” Proc. of the IEEE Int. Conf. on Robotics & Automation, pp. 539-544, 1996.

[4] J. E. Colgate, G. G. Schenkel, “Passivity of a Class of Sampled-Data Systems: Application to Haptic Interfaces,” Journal of Robotic Systems, Vol. 14, pp. 37-47, 1997.

[5] J. Troccaz, S. Lavallee, E. Hellion, “A Passive Arm with Dynamic Constraints: A Solution to Safety Problems in Medical Robots?,” Proc. of the Int. Conf. On Systems, Man and Cybernetics, vol.3, pp. 166–171, 1993.

[6] H. Davis, W. J. Book, “Torque Control of a Redundantly Actuated Passive Manipulator,” Proc. of the American Control Conf., pp. 959-963, 1997.

[7] O. Schneider, J. Troccaz, O. Chavanon, D. Blin, “PADyC: a Synergistic Robot for Cardiac Puncturing,” Proc. of the IEEE Int. Conf. on Robotics & Automation, pp. 2883–2888, 2000.

[8] T. Yoshikawa, “Foundations of Robotics: Analysis and Control,” The MIT Press, 1990.